Lecture notes on topological insulators

Ming-Che Chang

Department of Physics, National Taiwan Normal University, Taipei, Taiwan

(Dated: February 16, 2025)

CONTENTS

I. SURFACE STATE OF TOPOLOGICAL INSULATOR

In semiconductors, charge carriers are populated around the minimal energy gap, say at $\mathbf{k}=0$. Therefore, for most purpose, it is sufficient to know the effective Hamiltonian near $\mathbf{k}=0$. Furthermore, since the Hamiltonian needs to respect the symmetry of the crystal, its form is restricted. With these, we will determine the low-energy effective Hamiltonian of the surface states.

A. Symmetry of Hamiltonian

Consider a crystal with point group symmetry G. Write the representations for a group element $g\in G$ in real space, Hilbert space, and Fock space as g, U_g, and D_g respectively. Take rotation as an example, g is just the usual 3×3 rotation matrix, U_g is the matrix that rotates the bases of the Hamiltonian, and D_g rotates operators. Under the operation of g, an annihilation operator transforms as (Fang *et al.*, 2013),

$$D_g c_\alpha(\mathbf{R}) D_g^{-1} = \sum_{\alpha\beta} U_{\alpha\beta} c_\beta(\mathbf{R}'), \quad \mathbf{R}' = \mathsf{g}\mathbf{R}, \tag{1.1}$$

in which α,β are orbital indices, $\mathbf{R}$ is a lattice vector, and g is a 3×3 matrix of transformation.

Fourier transformation gives

$$c_\alpha(\mathbf{k}) = \frac{1}{\sqrt{N}}\sum_{\mathbf{R}} c_\alpha(\mathbf{R}) e^{-i\mathbf{k}\cdot\mathbf{R}}. \tag{1.2}$$

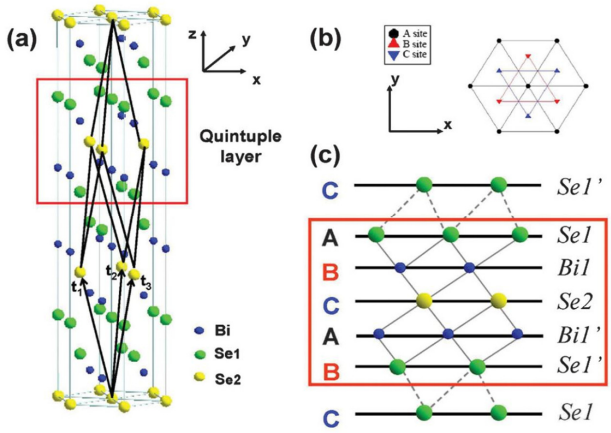

FIG. 1 (a) Crystal structure of Bi_2Se_3. (b) Top view of the (111)-surface. (c) Side view of the layered structure. Fig from Qi and Zhang, 2011.

It transforms as

$$\begin{aligned} D_g c_\alpha(\mathbf{k}) D_g^{-1} &= \frac{1}{\sqrt{N}}\sum_{\mathbf{R}}\sum_{\alpha\beta} U_{\alpha\beta} c_\beta(\mathbf{R}') \underbrace{e^{-i\mathbf{k}\cdot\mathbf{R}}}_{=e^{-i\mathbf{k}'\cdot\mathbf{R}'}} \\ &= \sum_{\alpha\beta} U_{\alpha\beta} c_\beta(\mathbf{k}'), \quad \mathbf{k}' = \mathsf{g}\mathbf{k}. \end{aligned} \tag{1.3}$$

Suppose the Hamiltonian is,

$$H = \sum_{\alpha,\beta} H_{\alpha\beta}(\mathbf{k}) c_\alpha^\dagger(\mathbf{k}) c_\beta(\mathbf{k}), \tag{1.4}$$

then the invariance under symmetry transformation requires

$$D_g H D_g^{-1} = H. \tag{1.5}$$

It follows that,

$$\mathsf{U}_g \mathsf{H}(\mathbf{k}) \mathsf{U}_g^{-1} = \mathsf{H}(\mathsf{g}\mathbf{k}). \tag{1.6}$$

B. Effective Hamiltonian of TI surface states

One can deduce the effective Hamiltonian for the surface states based on the consideration of symmetry. As an example, we consider the [111] surface state of Bi_2Te_3 (see Fig. 1). In addition to the TRS, there is also a C_{3v}

symmetry, which consists of a 3-fold rotation transformation C_3 and a mirror transformation $M : x \to -x$.

The operator for the 3-fold rotation is

$$C_3 = e^{i\pi/3\sigma_z}. \tag{1.7}$$

The mirror operation M needs to flip the signs of σ_y, σ_z, but preserve the sign of σ_x. Note that a mirror reflection in 3D equals an inversion followed by a 180° rotation. Therefore, $M^2 = -1$ for spin-1/2 electron (Kane, 2013). These restrictions give

$$M = i\sigma_x \tag{1.8}$$

The effective Hamiltonian is transformed as ($\Theta = i\sigma_y K$),

$$\begin{aligned} \Theta \mathsf{H}(\mathbf{k})\Theta^{-1} &= \mathsf{H}(-\mathbf{k}), & (1.9)\\ C_3 \mathsf{H}(k_\pm) C_3^{-1} &= \mathsf{H}(e^{\mp i2\pi/3} k_\pm), & (1.10)\\ M\mathsf{H}(k_\pm)M^{-1} &= \mathsf{H}(-k_\mp), & (1.11) \end{aligned}$$

where $\mathbf{k} = (k_x, k_y)$. Write the 2×2 Hamiltonian matrix as

$$\mathsf{H}(\mathbf{k}) = \begin{pmatrix} h(\mathbf{k}) & g(\mathbf{k}) \\ g^*(\mathbf{k}) & -h(\mathbf{k}) \end{pmatrix}, \tag{1.12}$$

then time-reversal symmetry dictates that $h(-\mathbf{k}) = -h(\mathbf{k}), g(-\mathbf{k}) = -g(\mathbf{k})$.

Rotation symmetry gives

$$\begin{aligned} h(k_\pm) &= h(e^{\mp 2\pi i/3} k_\pm); & (1.13)\\ e^{i2\pi/3} g(k_\pm) &= g(e^{\mp 2\pi i/3} k_\pm). & (1.14) \end{aligned}$$

Mirror symmetry gives

$$\begin{aligned} h(k_\pm) &= -h(-k_\mp); & (1.15)\\ g(k_\pm) &= g^*(-k_\mp). & (1.16) \end{aligned}$$

To linear order of the momentum, it is not difficult to see that $h(\mathbf{k}) = 0, g(\mathbf{k}) = ik_-$. Therefore,

$$\mathsf{H}(\mathbf{k}) = \varepsilon_0(k) + v(\sigma_x k_y - \sigma_y k_x). \tag{1.17}$$

To the third order of momentum, it is left as an exercise to show that

$$\mathsf{H}(\mathbf{k}) = \varepsilon_0(k) + v_k(\sigma_x k_y - \sigma_y k_x) + \frac{\lambda}{2}\left(k_+^3 + k_-^3\right)\sigma_z, \tag{1.18}$$

where $v_k = v_0(1 + \alpha k^2)$. The energy dispersion is

$$\varepsilon_\pm(\mathbf{k}) = \varepsilon_0(k) \pm \sqrt{v_k^2 k^2 + \lambda^2 k^6 \cos^2(3\theta)}, \tag{1.19}$$

where $\theta = \angle(\mathbf{k}, \hat{x})$. This would give a Fermi contour with 6-fold rotation symmetry (Fu, 2009), which is consistent with observation (Xu *et al.*, 2011).

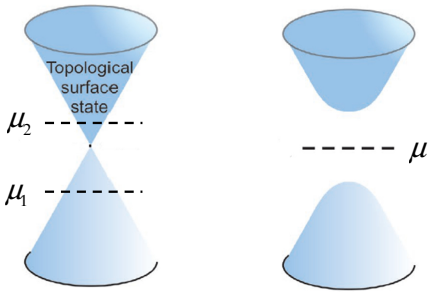

FIG. 2 (a) Dirac cone of the surface state. The chemical potential can be below (μ_1) or above (μ_2) the Dirac point. (b) The Dirac point can be opened by magnetization.

C. Berry curvature near level crossing

The 2D surface states of 3D TI have Dirac points in energy spectrum, similar to those of graphene's. A typical TI surface state Hamiltonian near a Dirac point is

$$\begin{aligned} \mathsf{H}_{SS} &= \alpha(\boldsymbol{\sigma} \times \mathbf{k})_z + O(k^2) & (1.20)\\ &\simeq \mathbf{h}(\mathbf{k}) \cdot \boldsymbol{\sigma}, & (1.21) \end{aligned}$$

where $\mathbf{h}(\mathbf{k}) = \alpha\mathbf{k} \times \hat{z} = \alpha(k_y, -k_x, 0)$. Again te spins of the electrons on the Fermi circles are parallel or anti-parallel to the field $\mathbf{h}(\mathbf{k})$. Hence after circling the Fermi circle once, an electron acquires a Berry phase $\gamma_\pm = \mp\pi$ for upper/lower band.

As in graphene, the value of the Berry phase $\gamma_C = \pi$ is protected by time-reversal symmetry, and the Berry curvature is a delta function

$$F_z^\pm(\mathbf{k}) = \mp\pi\delta^2(\mathbf{k}). \tag{1.22}$$

Due to the phase shift of π for a closed path, one expects to see **weak anti-localization**, instead of **weak localization**, in a graphene or a TI surface with disorders (He *et al.*, 2011). However, real samples are more complicated. Depending on condition, both types of localization can be observed (Lu and Shen, 2014; Tikhonenko *et al.*, 2009).

The Hall conductivity is given by,

$$\sigma_H = \frac{e^2}{h}\frac{1}{2\pi}\left(\int_{\text{filled}} d^2k F_z^+ + \int_{\text{filled}} d^2k F_z^-\right). \tag{1.23}$$

It's not difficult to see that the Hall conductivity is zero, no matter whether the chemical potential is located below or above the Dirac point (see Fig. 2(a)).

The Dirac point can be opened by magnetic dopants with magnetization m (see Fig. 2(b)),

$$\mathsf{H}_{SS} = \alpha(\boldsymbol{\sigma} \times \mathbf{k})_z + m\sigma_z, \tag{1.24}$$

which has the Berry curvature,

$$F_z^\pm = \mp\frac{\alpha^2 m}{2(m^2 + \alpha^2 k^2)^{3/2}}. \tag{1.25}$$

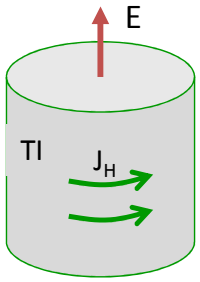

FIG. 3 A cylindrical topological insulator in an uniform electric field has a circulating surface Hall current.

If the chemical potential is inside the energy gap, the Hall conductivity is a half-integer,

$$\sigma_H = \frac{e^2}{h}\frac{1}{2\pi}\int d^2k F_z^- = \frac{1}{2}\frac{e^2}{h}. \tag{1.26}$$

Even though the TI has odd number of Dirac point on one surface, the total number of Dirac point for all surfaces should be even. Overall they would contribute an integer Hall conductivity.

D. Electromagnetic response of surface state

1. Magneto-electric coupling

Consider a cylindrical bar of topological insulator as shown in Fig. 3. Assuming that the Dirac point of the SS is *gapped by a TRS-breaking perturbation*, and *the chemical potential is inside the gap*, so that the SS has half-integer Hall conductance. If one applies an electric field along the z-axis of the cylinder, then on the surface there would be a circulating Hall current $j_H = (e^2/2h)E$. According to one of Ampere's theorem (Zangwill, 2013), the magnetic field produced by such a surface current is equivalent to that of an effective magnetization along the z-axis (in Gaussian units),

$$M = \frac{1}{c}j_H = \frac{e^2}{2hc}E. \tag{1.27}$$

Notice that M is proportional to E, instead of B. This is an example of **magneto-electric coupling**.

The thermodynamic potential for magneto-electric coupling is $U = -\chi_{ij}E_iB_j$ (see Sec. 51 of Landau and Lifshitz, 1984). This gives

$$P_i = -\frac{\partial U}{\partial E_i} = \chi_{ij}B_j, \tag{1.28}$$

$$M_j = -\frac{\partial U}{\partial B_j} = \chi_{ij}E_i. \tag{1.29}$$

Further differentiation gives

$$\chi_{ij} = \frac{\partial M_j}{\partial E_i} = \frac{\partial P_i}{\partial B_j}, \tag{1.30}$$

in which χ_{ij} is *not* required to be symmetric. Following Eq. (1.27), one has

$$P = \frac{e^2}{2hc}B. \tag{1.31}$$

For a heuristic explanation of the polarization induced by a magnetic field, see related discussion in Nomura, 2013.

Such a magneto-electric coupling can be obtained by adding a term $\mathcal{L}_\theta$ to the Lagrangian density of electromagnetic field (Qi *et al.*, 2009),

$$\mathcal{L}_{EM} = \frac{1}{8\pi}(E^2 - B^2) + \mathcal{L}_\theta - \rho\phi + \frac{1}{c}\mathbf{j}\cdot\mathbf{A}, \tag{1.32}$$

where

$$\mathcal{L}_\theta = \frac{e^2}{2hc}\mathbf{E}\cdot\mathbf{B} = \alpha\frac{\theta}{4\pi^2}\mathbf{E}\cdot\mathbf{B}, \tag{1.33}$$

$\alpha = e^2/\hbar c$ is the fine structure constant, and the **axion angle** $\theta = \pi$. The coupling strength $e^2/2h$ has its origin in the half-integer Hall effect.

We now introduce the 4-vector notation. Recall that

$$x^\mu = (ct, \mathbf{x}), \tag{1.34}$$

$$\partial^\mu = \left(\frac{\partial}{c\partial t}, -\frac{\partial}{\partial \mathbf{x}}\right), \tag{1.35}$$

$$j^\mu = (c\rho, \mathbf{j}), \tag{1.36}$$

$$A^\mu = (\phi, \mathbf{A}). \tag{1.37}$$

The electromagnetic field tensor is (see Chaps 11, 12 of Jackson, 1999),

$$F^{\mu\nu} \equiv \partial^\mu A^\nu - \partial^\nu A^\mu \tag{1.38}$$

$$= \begin{pmatrix} 0 & -E^1 & -E^2 & -E^3 \\ E^1 & 0 & -B^3 & B^2 \\ E^2 & B^3 & 0 & -B^1 \\ E^3 & -B^2 & B^1 & 0 \end{pmatrix}, \tag{1.39}$$

with a dual tensor,

$$\tilde{F}^{\mu\nu} \equiv \frac{1}{2}\epsilon^{\mu\nu\delta\sigma}F_{\delta\sigma} \tag{1.40}$$

$$= \begin{pmatrix} 0 & -B^1 & -B^2 & -B^3 \\ B^1 & 0 & E^3 & -E^2 \\ B^2 & -E^3 & 0 & E^1 \\ B^3 & E^2 & -E^1 & 0 \end{pmatrix}. \tag{1.41}$$

It follows that,

$$F^{\mu\nu}F_{\mu\nu} = -2(E^2 - B^2), \tag{1.42}$$

$$\frac{1}{2}\epsilon^{\mu\nu\delta\sigma}F_{\mu\nu}F_{\delta\sigma} = -4\mathbf{E}\cdot\mathbf{B}. \tag{1.43}$$

Therefore,

$$\mathcal{L}_{EM} = -\frac{1}{16\pi}F^{\mu\nu}F_{\mu\nu} + \mathcal{L}_\theta - \frac{1}{c}j^\mu A_\mu, \tag{1.44}$$

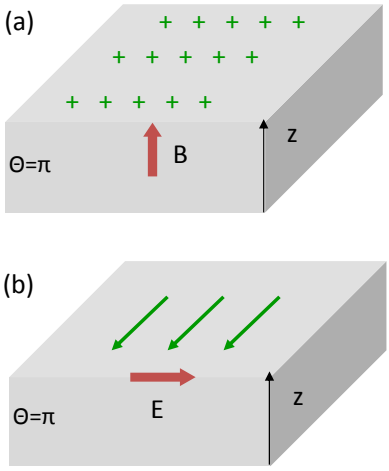

FIG. 4 (a) A magnetic field induces electric charges on the surface of a TI. (b) An electric field induces a Hall current on the surface of a TI.

and the axion term is

$$\mathcal{L}_\theta = -\alpha\frac{\theta}{16\pi^2}\frac{1}{2}\epsilon^{\mu\nu\delta\sigma}F_{\mu\nu}F_{\delta\sigma} \quad (1.45)$$

$$= -\alpha\frac{\theta}{16\pi^2}\epsilon^{\mu\nu\delta\sigma}\partial_\mu(A_\nu F_{\delta\sigma}), \quad (1.46)$$

which is a total derivative *if* the axion angle is uniform throughout the whole space.

Using the Euler-Lagrange equation of motion,

$$\frac{\partial\mathcal{L}_{EM}}{\partial A_\nu} - \partial_\mu\frac{\partial\mathcal{L}_{EM}}{\partial(\partial_\mu A_\nu)} = 0, \quad (1.47)$$

we have,

$$\partial_\mu\left(F^{\mu\nu} + \alpha\frac{\theta}{\pi}\tilde{F}^{\mu\nu}\right) = \frac{4\pi}{c}j^\nu. \quad (1.48)$$

Also, from Eq. (1.38), we have

$$\partial_\mu F_{\nu\lambda} + \partial_\nu F_{\lambda\mu} + \partial_\lambda F_{\mu\nu} = 0. \quad (1.49)$$

These two are Maxwell equations in relativistic covariant form.

2. Axion electrodynamics

When written in $\mathbf{E},\mathbf{B}$ fields, the Maxwell equations are,

$$\nabla\cdot\left(\mathbf{E} + \alpha\frac{\theta}{\pi}\mathbf{B}\right) = 4\pi\rho, \quad (1.50)$$

$$\nabla\times\left(\mathbf{B} - \alpha\frac{\theta}{\pi}\mathbf{E}\right) = \frac{4\pi}{c}\mathbf{j} + \frac{1}{c}\frac{\partial}{\partial t}\left(\mathbf{E} + \alpha\frac{\theta}{\pi}\mathbf{B}\right), \quad (1.51)$$

$$\nabla\cdot\mathbf{B} = 0, \quad (1.52)$$

$$\nabla\times\mathbf{E} = -\frac{1}{c}\frac{\partial}{\partial t}\mathbf{B}. \quad (1.53)$$

One can move the axion terms to the right hand side of the equations, such that

$$\nabla\cdot\mathbf{E} = 4\pi(\rho+\rho_\theta), \quad (1.54)$$

$$\nabla\times\mathbf{B} = \frac{4\pi}{c}(\mathbf{j}+\mathbf{j}_\theta) + \frac{1}{c}\frac{\partial\mathbf{E}}{\partial t}, \quad (1.55)$$

$$\text{where}\quad \rho_\theta = -\frac{\alpha}{4\pi^2}\nabla\cdot(\theta\mathbf{B}), \quad (1.56)$$

$$\mathbf{j}_\theta = \frac{\alpha c}{4\pi^2}\nabla\times(\theta\mathbf{E}) + \frac{\alpha}{4\pi^2}\frac{\partial}{\partial t}(\theta\mathbf{B}). \quad (1.57)$$

We put θ inside the differentiation, since it is not uniform throughout the whole space: π inside a TI, but 0 outside.

Assume the semi-infinite space below xy-plane is occupied by a TI, such that $\theta(z) = \pi h(-z)$, where $h(z)$ is the Heaviside step function. If one applies an uniform magnetic field along the z-axis (see Fig. 4(a)), then the axion-induced effective charge is,

$$\rho_\theta = \frac{\alpha}{4\pi}\delta(z)B_z. \quad (1.58)$$

That is, there is a thin layer of charges on the surface of the TI. This is consistent with Eq. (1.31).

On the other hand, if one applies an uniform electric field parallel to the surface (see Fig. 4(b)), the the axion-induced effective current density is,

$$\mathbf{j}_\theta = -\frac{\alpha c}{4\pi}\delta(z)\hat{z}\times\mathbf{E}. \quad (1.59)$$

That is, the is a thin layer of current on the surface of the TI, perpendicular to the E-field. This is a Hall current with Hall conductivity $\sigma_H = \alpha c/4\pi = e^2/2h$. Thus, the axion term does produce correct electromagnetic responses of the TI surface state.

In the dynamical range, the magneto-electric coupling would rotate the polarization plane of an optical wave transmitted though (**Faraday effect**) and reflected from (**Kerr effect**) the TI surface (Tse and MacDonald, 2010; Wu *et al.*, 2016). Such rotations are related to the surface Hall current induced by the electric field of the optical wave. Similar effect has been observed in graphene, because it can also have the surface Hall current (Crassee *et al.*, 2011).

3. Axion angle and Berry connection

The axion angle is a coarse-grained description of the electromagnetic response of TI. Like electric permittivity and magnetic permeability, it is a response function that depends on material property. In principle, χ_{ij} can be calculated from the theory of response using Eq. (1.30). This difficult task has been accomplished by Vanderbilt's group (Essin *et al.*, 2010; Malashevich *et al.*, 2010). They showed that the general form of the **magneto-electric susceptibility** is,

$$\chi_{ij} = \tilde{\chi}_{ij} + \chi_\theta\delta_{ij}, \quad (1.60)$$

in which the second term, $\chi_\theta = \frac{e^2}{2hc}\frac{\theta}{\pi}$, is related to the magneto-electric coupling in previous section. The axion angle is given as an integral of Berry connections,

$$\theta = \frac{1}{4\pi}\int_{BZ} d^3k\ \epsilon_{abc}\mathrm{tr}\left(\mathsf{A}_a\partial_b\mathsf{A}_c - \frac{2i}{3}\mathsf{A}_a\mathsf{A}_b\mathsf{A}_c\right). \quad (1.61)$$

The trace is a sum over occupied energy bands, and

$$[\mathsf{A}_a(\mathbf{k})]_{nn'} = i\langle u_{n\mathbf{k}}|\frac{\partial}{\partial k_a}|u_{n'\mathbf{k}}\rangle. \quad (1.62)$$

It can be proved that, with TRS, the axion angle is defined only up to $2\pi w, w \in Z$.

The reason that the integrand of the axion angle is the **Chern-Simons term** can be understood from the perspective of dimensional reduction. That is, the 3D TI can be considered as a descendent of the 4D quantum Hall effect, which is characterized by the second Chern number (Qi *et al.*, 2008).

Exercise

1. Following the discussion in subsection B, generalize the effective Hamiltonian of the TI surface state to the third order of momentum,

$$\mathsf{H}(\mathbf{k}) = \varepsilon_0(k)+v_k(\sigma_x k_y-\sigma_y k_x)+\frac{\lambda}{2}\left(k_+^3+k_-^3\right)\sigma_z. \quad (1.63)$$

2. For the 2DEG in an asymmetric quantum well, there can be **Rashba spin-orbit coupling**. The Hamiltonian is,

$$\mathsf{H}(\mathbf{k}) = \frac{\hbar^2k^2}{2m^*} + \alpha\left(\boldsymbol{\sigma}\times\mathbf{k}\right)\cdot\hat{z}, \quad (1.64)$$

where α is the strength of the Rashba coupling, and z is the direction perpendicular to the 2DEG.
(a) Obtain and plot the energy spectrum $E(|\mathbf{k}|)$, which has two paraboloids with a point degeneracy at $k = 0$.
(b) Find out the Berry curvature of the degenerate point.
3. Following Prob. 2.
(a) What is the Hall conductivity when the chemical potential μ is higher or lower than the nodal energy?
(b) If the 2DEG is doped with magnetization m, then

$$\mathsf{H}(\mathbf{k}) = \frac{\hbar^2k^2}{2m^*} + \alpha\left(\boldsymbol{\sigma}\times\mathbf{k}\right)\cdot\hat{z} + m\sigma_z. \quad (1.65)$$

When the chemical potential is inside the gap, show that (k_F is the Fermi wave vector)

$$\sigma_H = \frac{1}{2}\frac{e^2}{h}\left(1-\frac{m}{\sqrt{m^2+\alpha^2k_F^2}}\right). \quad (1.66)$$

4. (a) Starting from the Lagrangian density $\mathcal{L}_{EM}$, and using the Euler-Lagrange equation, derive the Maxwell equation in Eq. (1.48).
(b) Verify Eq. (1.49), which by the way is related to the **Bianchi identity** in differential geometry.
(c) Show that the Maxwell equations in conventional form are given as Eqs. (1.50), (1.51), (1.52), (1.53).

REFERENCES

Crassee, Iris, Julien Levallois, Andrew L. Walter, Markus Ostler, Aaron Bostwick, Eli Rotenberg, Thomas Seyller, Dirk van der Marel, and Alexey B. Kuzmenko (2011), "Giant faraday rotation in single- and multilayer graphene," Nat Phys **7** (1), 48–51.

Essin, Andrew M, Ari M. Turner, Joel E. Moore, and David Vanderbilt (2010), "Orbital magnetoelectric coupling in band insulators," Phys. Rev. B **81**, 205104.

Fang, Chen, Matthew J. Gilbert, and B. Andrei Bernevig (2013), "Entanglement spectrum classification of C_n-invariant noninteracting topological insulators in two dimensions," Phys. Rev. B **87**, 035119.

Fu, Liang (2009), "Hexagonal warping effects in the surface states of the topological insulator bi_2te_3," Phys. Rev. Lett. **103**, 266801.

He, Hong-Tao, Gan Wang, Tao Zhang, Iam-Keong Sou, George K. L Wong, Jian-Nong Wang, Hai-Zhou Lu, Shun-Qing Shen, and Fu-Chun Zhang (2011), "Impurity effect on weak antilocalization in the topological insulator bi_2te_3," Phys. Rev. Lett. **106**, 166805.

Jackson, J D (1999), *Classical Electrodynamics* (John Wiley and Sons, Inc.).

Kane, CL (2013), "Chapter 1 - topological band theory and the 2 invariant," in *Topological Insulators*, Contemporary Concepts of Condensed Matter Science, Vol. 6, edited by Marcel Franz and Laurens Molenkamp (Elsevier) pp. 3 – 34.

Landau, L D, and E. M. Lifshitz (1984), *Electrodynamics of continuous media*, 2nd ed., Course of theoretical physics No. 8 (Butterworth-Heinemann).

Lu, Hai-Zhou, and Shun-Qing Shen (2014), "Weak localization and weak anti-localization in topological insulators," Proc.SPIE **9167**, 9167.

Malashevich, Andrei, Ivo Souza, Sinisa Coh, and David Vanderbilt (2010), "Theory of orbital magnetoelectric response," New Journal of Physics **12** (5), 053032.

Nomura, K (2013), "Fundamental theory of topological insulator," Unpublished, written in Japanese.

Qi, Xiao-Liang, Taylor L. Hughes, and Shou-Cheng Zhang (2008), "Topological field theory of time-reversal invariant insulators," Phys. Rev. B **78**, 195424.

Qi, Xiao-Liang, Rundong Li, Jiadong Zang, and Shou-Cheng Zhang (2009), "Inducing a magnetic monopole with topological surface states," Science **323** (5918), 1184–1187.

Qi, Xiao-Liang, and Shou-Cheng Zhang (2011), "Topological insulators and superconductors," Rev. Mod. Phys. **83**, 1057–1110.

Tikhonenko, F V, A. A. Kozikov, A. K. Savchenko, and R. V. Gorbachev (2009), "Transition between electron localization and antilocalization in graphene," Phys. Rev. Lett. **103**, 226801.

Tse, Wang-Kong, and A. H. MacDonald (2010), "Giant magneto-optical kerr effect and universal faraday effect in thin-film topological insulators," Phys. Rev. Lett. **105**, 057401.

Wu, Liang, M. Salehi, N. Koirala, J. Moon, S. Oh, and N. P. Armitage (2016), "Quantized faraday and kerr rotation and axion electrodynamics of a 3d topological insulator," Science **354** (6316), 1124–1127.

Xu, Su-Yang, Y. Xia, L. A. Wray, S. Jia, F. Meier, J. H. Dil, J. Osterwalder, B. Slomski, A. Bansil, H. Lin, R. J. Cava,

and M. Z. Hasan (2011), "Topological phase transition and texture inversion in a tunable topological insulator," Science **332** (6029), 560–564.

Zangwill, Andrew (2013), *Modern electrodynamics* (Cambridge Univ. Press, Cambridge).